EUROPEAN ORGANIZATION FOR NUCLEAR RESEARCH

European Laboratory for Particle Physics

Large Hadron Collider Project **LHC Project Report 172**

LHC main dipoles proposed baseline current ramping

L. Bottura, P. Burla and R.Wolf

Abstract

Several studies performed from 1994 to 1996 including some in the framework of the Dynamic Effects Working Group, have shown that the magnitude of the magnetic field imperfections generated in the LHC main dipoles depends partly on the shape of the magnetic field ramp. A current ramp optimisation has been carried out with several combinations of mathematical functions. The result of this study is the proposed baseline current ramp. The graphic representation of this ramp is included in this report. Theoretical dynamic errors expected with this ramp are compared with those produced with a straight ramp at constant current rate, thus demonstrating the improvement obtained. A set of formulae and parameters required for the actual calculation of the baseline ramp is given in the Appendix.

LHC Division

Administrative Secretariat
LHC Division
CERN
CH - 1211 Geneva 23
Switzerland

Geneva, 23 March 1998

1. Introduction

The dynamic field distortions in the LHC superconducting magnets are generated, among others, under the following circumstances:

– During a constant current plateau, the magnetisation of the superconducting cable in the magnet decays slowly. When ramping resumes, the long-term magnetization changes recover to almost their initial value after a very small field change. The result is a rapid change of field and field errors in the magnet (snap-back).

– While ramping, interstrand coupling currents in the superconducting cables produce dynamic field imperfections.

A contribution to minimising such errors can be achieved by carefully choosing the shape of the magnet current ramp.

The current ramp should minimise errors and therefore make it easier to correct dynamically field imperfections. The criteria retained for the construction of such a ramp are discussed and basic equations defining the various segments of the current ramp are given.

2. Basic assumptions

For the calculations included in this document it is assumed that:

– Current and magnetic field are fully proportional (no saturation effects).

$$I(t) = Sc \cdot B(t)$$

I(t): Current value @ time t |A|

B(t): Field value @ time t |T|

Sc : Proportionality (scaling) factor |A/T|

– The theoretical "dynamic resistance" can be neglected as long as the energy stored in the cryogenic bus-bar is negligible compared to the energy stored in the magnets. The superconducting bus-bar and magnet string resistance is then considered to be zero, and the resistance Rw of the warm connections from the power converter to the feed-box can be considered as the only resistance in the circuit.

– The time variable t appearing in each segment equation is always relative to the start of the segment ($t = 0$).

– The ramp description which follows deals only with the "beam-in" portion of the full current cycle. The ramp-down calculation (from the nominal current down to the set -up of the injection plateau) is not described.

– The injection plateau at constant current I_{inj}, is defined as the **first segment of the current ramp**.

$$\underline{\underline{I_1(t) = I_{inj}(t)}}$$

3. Ramping considerations

3.1. Start of ramping

In proper power-converter operation it is important to avoid abrupt voltage discontinuities.

The first derivative of the current ramp function I(t) applied to a magnet is directly proportional to the voltage across this magnet:

$$U_{mag} = L_{mag} \cdot I'(t)$$

U_{mag}: Magnet voltage |V|

L_{mag}: Magnet inductance |V*s/A|

I'(t): First derivative of I(t) |A/s|

If the derivative I'(t) does not have a zero value at the start of ramping, the generation of a current ramp function having such a derivative would require a voltage discontinuity.

Therefore, the first condition to be fulfilled by the current ramp function I(t) is that the first derivative I'(t) at the ramping start should be zero.

On the other hand, it has been shown [4] that if I'(t) is kept low at the end of the snap-back, the bandwidth of the control system required to dynamically correct this error can be substantially reduced.

These two conditions will be met with a **second segment of the current ramp** function which follows a quadratic parabola up to the junction with the next segment and which must occur after the end of the snap-back:

$$\underline{\underline{I_2(t) = I_{inj}(1 + \alpha \cdot t^2)}}$$

I_{inj}: Injection current; second segment initial current value |A|

α : Quadratic coefficient |1/s^2|

t: Time |s| relative to segment start.

The first derivative of this expression $I'(t) = 2 \cdot I_0 \cdot \alpha \cdot t$ has a value of zero when t=0 meeting the above condition.

It should be noted that some parameters belonging to the *next exponential segment* must be known at this point in order to calculate the required parameters that fully define this segment (see Appendix, section A-1.2).

3.2. Ramping criteria

In previous studies [1], [2] and [3], the relative magnetic field error produced by interstrand coupling currents has been widely commented. In summary, the magnetic field error produced by interstrand coupling current (and by other types of eddy currents) is proportional to the ramp rate B' (t). Therefore, at a constant ramp rate the relative field error b_{i-cpl} is highest at low fields.

$$b_{i\_cpl} = C_c \cdot \frac{B'(t)}{B(t)}$$

b_{i_cpl}: Relative coupling current error of order i. |Units|

C_c: Coupling current coefficient |Units*s|

The magnitude of this error can be optimised to be constant if the magnetic field ramp function B(t) is an exponential while ramping in such a way that with

$$B(t) = B_0 \cdot e^{\beta \cdot t}$$

and

$$B'(t) = \beta \cdot B_0 \cdot e^{\beta \cdot t}$$

B_0: Initial magnetic field value |T|

β : Inverse of the field function time constant |1/s|

B(t): Magnetic field |T|

B'(t): First derivative of magnetic field |T/s|

the expression of the relative error due to interstrand coupling currents becomes

$$b_{i\_cpl} = \beta \cdot C_c \ .$$

Thus the value of b_{i_cpl} is constant as long as the magnetic field ramp follows an exponential function.

Therefore, according to the assumption made (magnetic field and current are proportional) in order to minimise the interstrand coupling currents error while ramping, the **third segment of the current ramp** should be an exponential function:

$$\underline{\underline{I_3(t) = I_{exp\_init} \cdot e^{\beta \cdot t}}}$$

I_{exp_init} : Third segment current initial value |A|

β : Inverse of the current function time constant |1/s|

3.3. Voltage limit during ramping

The current ramping will follow an exponential function up to a suitable value of magnetic field, B_{exp_max}=3 T, produced by the current I_{exp_max} and identified in [1] as giving a reasonably low ramping time.

This field must be reached when the power converter delivers nearly the maximum output voltage whereas the current rate hits the maximum value $I'(t)_{max}$ which can be delivered by the power converter.

From this point on, the **fourth segment of the current ramp** equation becomes a straight linear ramp with constant current-rate at the maximum allowed.

$$I_4(t) = I_{exp\_max} + I'(t)_{max} \cdot t$$

I_{exp_max}: Fourth segment initial current value, producing B_{exp_max} |A|

$I'(t)_{max}$: Maximum current rate available |A/s|

3.4. Flat-top settling

In order to preserve the "magnetic history" of the magnets it is not permitted to reverse the sign of the current-rate during the period of the beam-in part of the current cycle, including the injection plateau. It is therefore of primary importance that no current overshoot takes place neither during the injection plateau nor the flat-top settling.

On the other hand, but for the same reason, the current ramp function should reach the flat-top level with a first derivative value of zero.

This can be achieved by stopping the linear ramp at a current value a few percent lower than the flat-top. From this point up to the flat-top the **fifth segment of the current ramp** equation should be a settling quadratic parabola.

$$\underline{\underline{I_5(t) = I_{flt} + \gamma \cdot t^2}}$$

I_{flt}: Flat-top current (end value), fifth segment final value |A|

γ : Current gradient during flat-top settling |A/s²|

t : Time |s|

4. Baseline LHC current ramp for Main Dipole

4.1. Ramp parameters definition

The numerical values of the basic parameters used to calculate the ramp are shown below.

Basic parameters

Given values:

Nominal magnetic field	B_{nom}	=	8.4	|T|
Minimum magnetic field (hysteresis compens.)	B_{hys}	=	0.25	|T|
Injection plateau magnetic field	B_{inj}	=	0.54	|T|
Nominal current	I_{nom}	=	11500	|A|
Magnet inductance	L_{mag}	=	16.63	|Hy|
Warm current leads resistance	R_{w}	=	$8.7 \cdot 10^{-4}$	|Ω|
Injection plateau Current	I_{inj}	=	739.29	|A|
Minimum current (hysteresis compens.)	I_{hys}	=	342.26	|A|
Current variation @ end of snap-back	ΔI_{sn_b}	=	20	|A|
Current rate @ end of snap-back	$I'(t)_{sn\_b}$	=	0.6	|A/s|
Maximum allowed current rate	$I'(t)_{max}$	=	10	|A/s|
Field @ end of exponential segment	B_{exp_max}	=	3	|T|

Calculated values:

Current to field scaling factor	$Sc = \frac{I_{nom}}{B_{nom}}$	=	$1.37 \cdot 10^{-3}$	|A/T|

These numerical values give, if used within the respective time intervals in the equations defined in the Appendix, sections A-1.1 to A-1.5, the "beam-in" ramp shown below.

The full current cycle shown in Fig. 1 is composed of:

a) Descending ramp, from the nominal current down to the setting-up of the injection plateau (not described in this report).

b) The described ramp, starting with the injection plateau up to the nominal current.

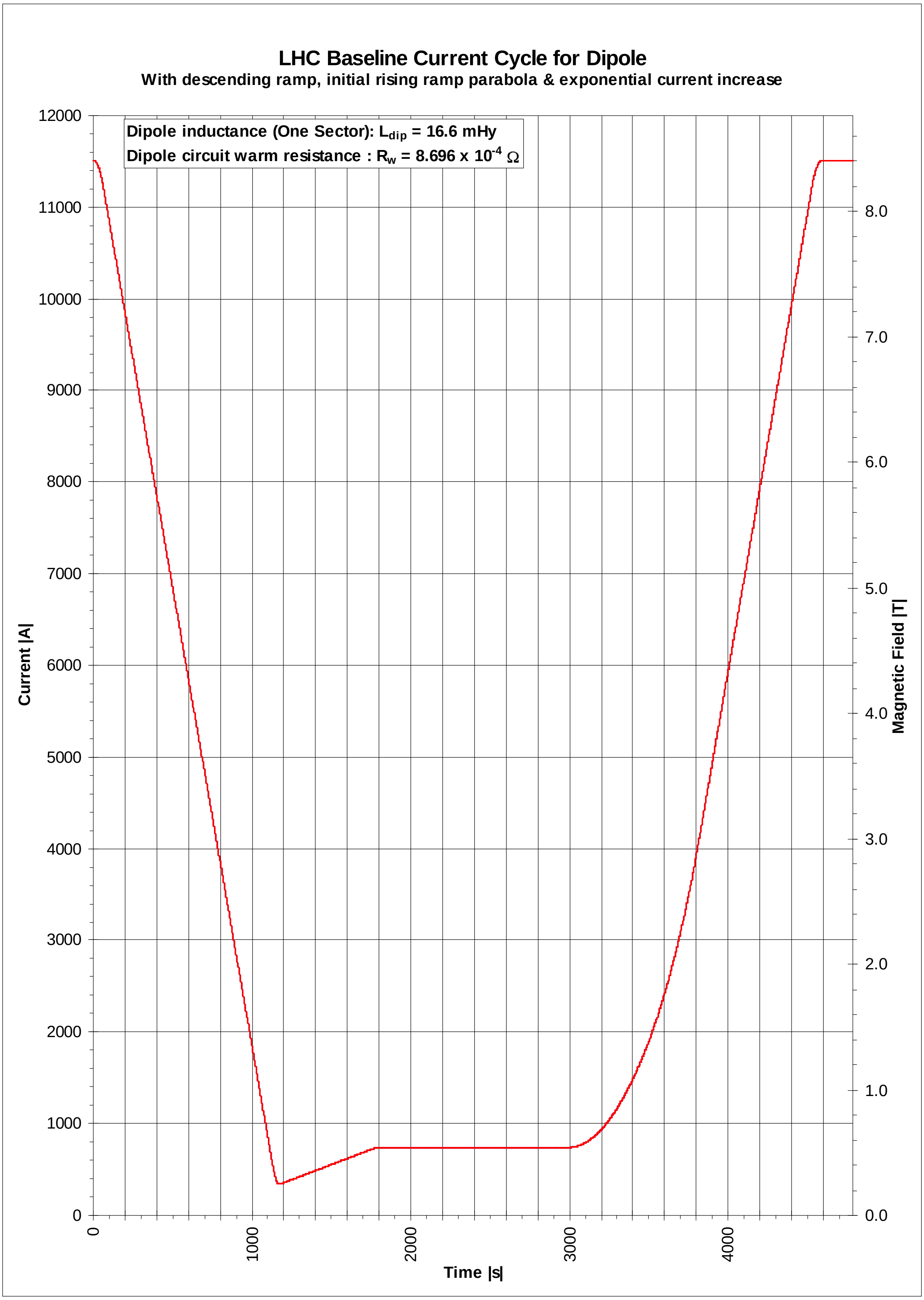

Fig. 1 - LHC baseline current cycle for dipole.

4.2. Ramp shape effect on dynamic errors

To demonstrate the current ramp shape influence on the relative error b_{3_cpl} (relative coupling currents sextupole error) a constant current rate ramp is shown in Fig. 2 together with the proposed baseline LHC ramp.

The expected errors due to interstrand coupling currents and produced by both ramps are calculated with the same parameters and by means of the model described in [4] and the error table in [5]. An example of the b_{3_cpl} error is shown in Fig. 3.

An improvement by a factor of 5 can be expected on the relative error magnitude with the proposed LHC baseline ramp compared to the simple straight ramp, at the expense of a seven minute increase in the ramping time.

Another important effect is the tune shift at the start of the ramp. This tune shift comes from the tracking error between quadrupoles and dipoles due to the change in their main component generated by interstrand coupling currents. Figure 4 gives an estimate using the values given in [5]. The tune shift is decreased by the same factor of 5, as above.

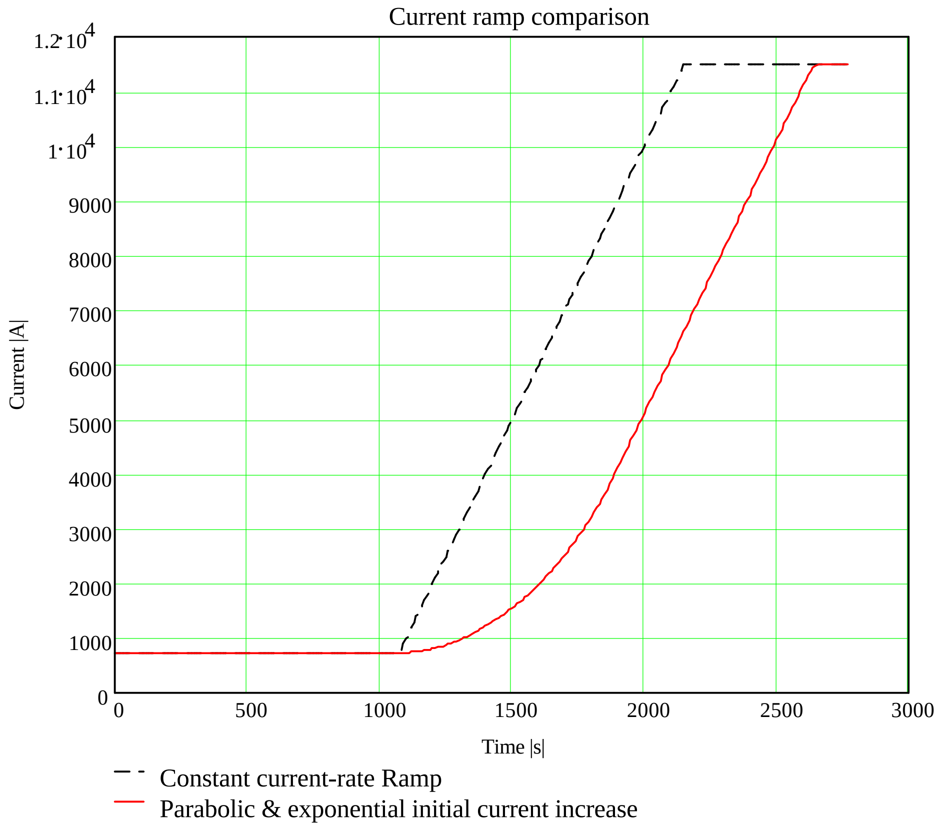

Fig. 2 - Linear ramp (10 A/s) and LHC baseline ramp compared.

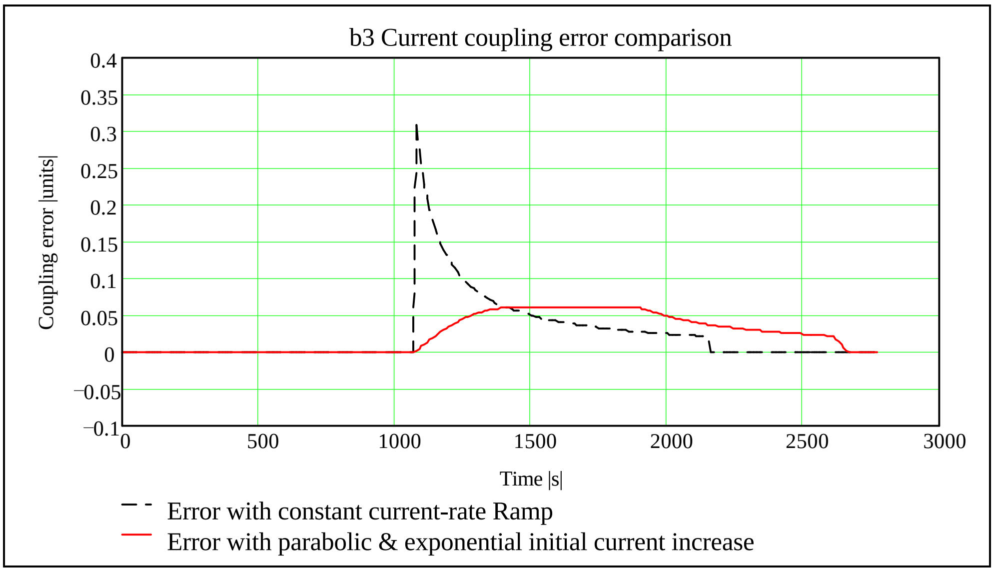

Fig. 3 - Calculated decrease of the field error b_{3_cpl} using the LHC baseline ramp. (Shown is the expected sextupole error computed from data given in [5].)

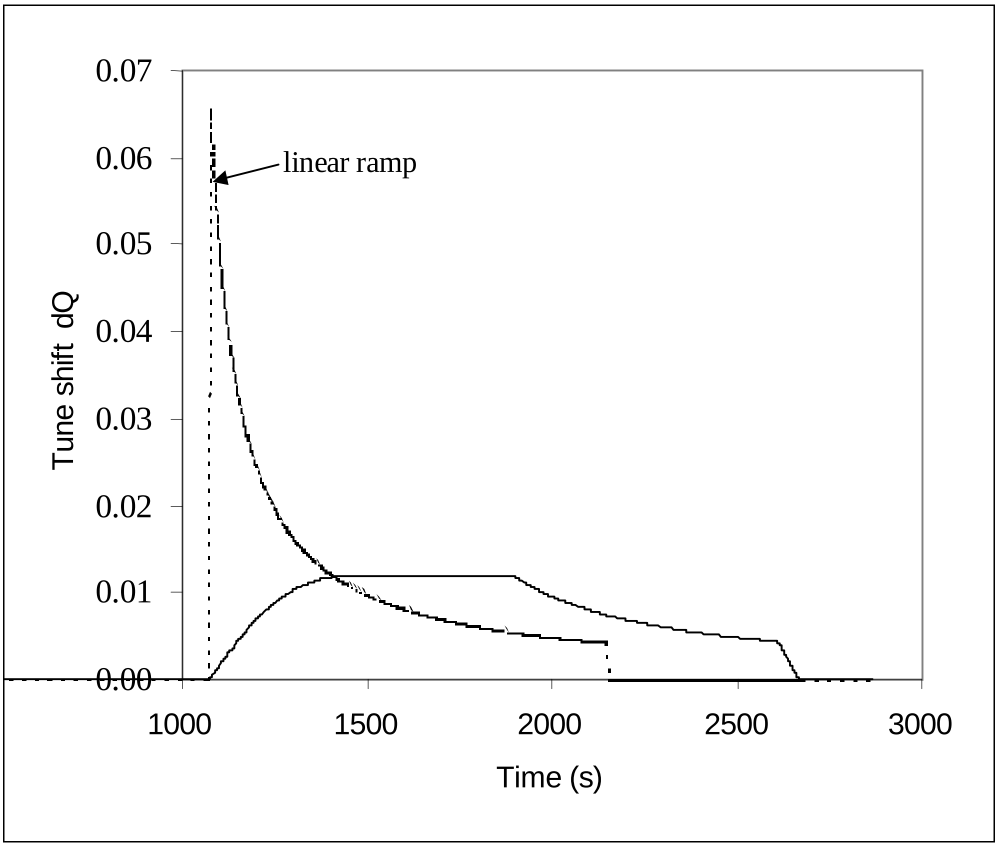

Fig. 4 - Tune shift due to interstrand eddy currents. Estimated with the change in the main components of main dipole and quadrupole given in [5].

4.3. Ramp shape effect on snap-back

The current rate after the injection point (t=1074 s), at the start of field increase, must be kept as low as possible in order to limit the rate of the decay recovery.

In Fig. 5 below, the expected shape difference of the decay recovery produced by a constant current-rate ramp and by the LHC baseline ramp can be seen. The rate of error change shown in Fig. 6 is of the order of 16 times slower with a soft start than with a straight ramp (-0.03 versus -0.45 Units/s).

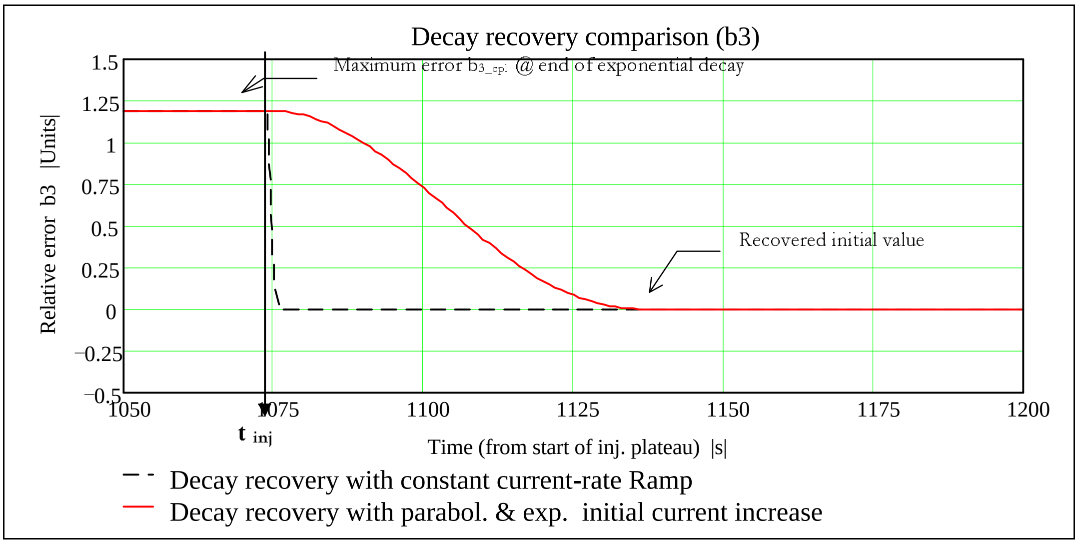

Fig. 5 - Snap-back of sextupole error due to magnetisation recovery at start of the ramp.

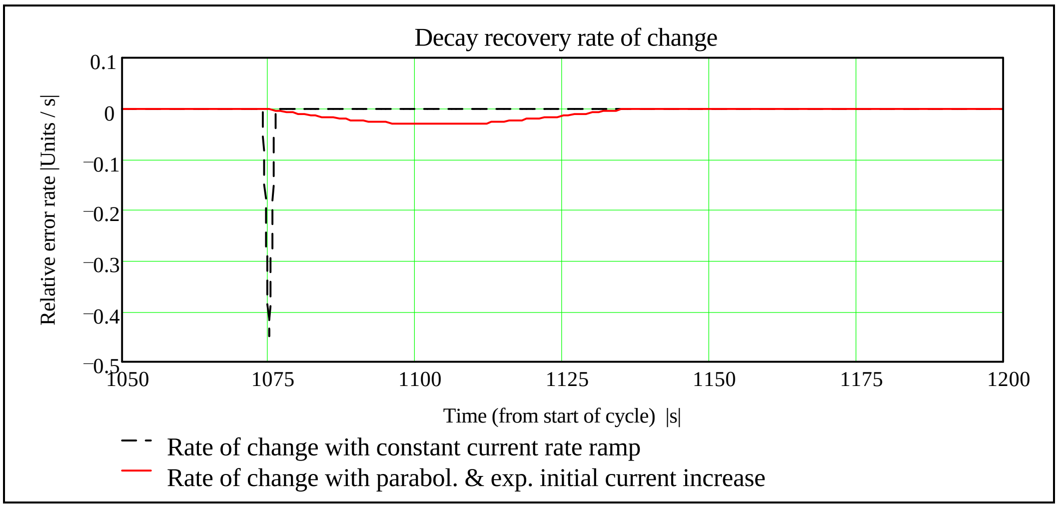

Fig. 6 - Calculated decrease (~16 x) of the field error rate of change during snap-back.

5. Conclusion

We have constructed a dipole current ramp that decreases the field errors due to eddy currents by a factor of 5. This is at the expense of an increase in ramp duration of 7 minutes, compared to a linear ramp with a total duration of 20 minutes.

This we think will allow to make field errors, due to interstrand currents, negligible provided that the interstrand resistance assumed in [5] can be obtained. An exception is the change in the main component of the dipole and quadrupole which gives a tune shift at the start of the ramp ($\delta Q \approx 0.012$).

In the "snap-back" recovery phase the rate of change of the field errors is diminished by a factor of 16. This gives an interval of about one minute in which to apply the necessary corrections. It remains to be seen if this is long enough.

Similar reductions in field errors and snap-back recovery rates are expected to occur in other magnets, notably the main quadrupoles.

Magnetic measurements with ramps of the type described here should be performed in the future to verify the predictions made above. This will also allow to establish which injection set-up procedure is best for limiting snap-back as much as possible.

References

[1] A.P. Verweij and R. Wolf, "Field errors due to interstrand coupling currents in the LHC dipoles and quadrupoles", CERN AT-MA/AV Internal Note 94-97, March, 1994.

[2] A. Faus-Golfe, "Minimization of the ramp-induced non-linear field imperfections in LHC", LHC Project Note 9, May, 1995.

[3] L. Bottura "Transfer function for field and field errors in the LHC prototype", private communication.

[4] P. Burla, "Simulation of transfer function for LHC dipoles", CERN, Dynamic Effects Working Group, Minutes of the 15th Meeting, December 6th, 1996.

[5] "LHC Main Dipole and Quadrupole Errors, Version 9712", CERN, Parameter & Layout Committee, Minutes of the 31st meeting, November 26th, 1997.

Appendix

Formulae and parameters for Current Ramp calculation

In order to allow the actual calculation of the current ramp, a complete set of formulae with the associated parameters is given below.

The basic parameters required to start the ramp calculation are the following:

Basic parameters:

Given values:

Nominal magnetic field	B_{nom}	|T|
Nominal current:	I_{nom}	|A|
Magnet inductance:	L_{mag}	|Hy|
Warm connection resistance:	R_{w}	|Ω|

Calculated values:

Current to field scaling factor:	$Sc = \frac{I_{nom}}{B_{nom}}$	|A/T|

A-1.1. First segment: Injection plateau

The injection plateau is the first segment of the current ramp.

Injection front porch:

Given values:

Injection current:	I_{inj}	| A |
Segment duration	Δt_{plat}	| s |

Time data for concatenation:

Absolute starting time	$t_0 = 0$	| s |
Absolute ending time	$t_{inj} = t_0 + \Delta t_{plat}$	| s |

First segment calculation:

Time interval of segment validity: $0 \le t \le \Delta t_{plat}$

A-1.2. Second segment: Parabolic start of ramping

Initial Parabola:		
Given values:		
Current variation during snap-back	ΔI_{sn_b}	|A|
Current rate @ end of Snap-back	$I'(t)_{sn\_b}$	|A/s|
Maximum allowed current rate	$I'(t)_{max}$	|A/s|
Field @ end of exponential segment	B_{exp_max} (see 3.1)	|T|
Calculated values:		
Current @ end of exponential segment	$I_{exp\_max} = B_{exp\_max} \cdot Sc$ (see 3.1)	|A|
Quadratic time coefficient	$\alpha = \dfrac{\left[I'(t)_{sn\_b}\right]^2}{4 \cdot I_{inj} \cdot \Delta I_{sn\_b}}$	|1/s²|
Parabolic segment duration	$\Delta t_{p1} = \dfrac{I_{exp\_max}}{I'(t)_{max}} - \sqrt{\left(\dfrac{I_{exp\_max}}{I'(t)_{max}}\right)^2 - \dfrac{1}{\alpha}}$	|s|
Current variation during segment	$\Delta I_{p1} = I_{inj} \cdot \alpha \cdot \Delta t_{p1}^2$	|A|
Time data for concatenation:		
Absolute starting time	t_{inj}	|s|
Absolute ending time	$t_{b\exp} = t_{inj} + \Delta t_{p1}$	|s|

Second segment calculation:

Time interval of segment validity: $0 \le t \le \Delta t_{p1}$

$$\boxed{I_2(t) = I_{inj} \cdot (1 + \alpha \cdot t^2)}$$

A-1.3. Third segment: Exponential current increase

Exponential ramping:

Given values:

None

Calculated values:

Initial current of exponential segment	$I_{exp\_init} = I_{inj} + \Delta I_{p1}$	|A|
Time constant inverse	$\beta = \dfrac{I'(t)_{end\_p1}}{I_{exp\_init}}$	|1/s|
Exponential segment duration	$\Delta t_{exp} = \dfrac{1}{\beta} \cdot \ln\left(\dfrac{I'(t)_{max}}{I'(t)_{end\_p1}}\right)$	|s|

Time data for concatenation:

Absolute starting time	$t_{b\exp}$	|s|
Absolute ending time	$t_{blin} = t_{b\exp} + \Delta t_{exp}$	|s|

Third segment calculation:

Time interval of segment validity: $0 \le t \le \Delta t_{p1}$

$$\boxed{I_3(t) = I_{exp\_init} \cdot e^{\beta \cdot t}}$$

A-1.4. Fourth segment: Linear current increase

Linear ramping:		
Given values:		
Initial current of linear segment	I_{exp_max}	|A|
Maximum allowed current rate	$I'(t)_{max}$	|A/s|
Flat top current	I_{flt}	|A|
Current variation during settling parabola	$\Delta I_{p2} = (n\%) * I_{flt}$	|A|
Calculated values:		
Current variation during segment	$\Delta I_{ramp} = \left(I_{flt} - \Delta I_{p2}\right) - I_{exp\_max}$	|A|
Linear segment duration	$\Delta t_{ramp} = \dfrac{\Delta I_{ramp}}{I'(t)_{max}}$	|s|
Time data for concatenation:		
Absolute starting time	t_{blin}	|s|
Absolute ending time	$t_{eramp} = t_{blin} + \Delta t_{ramp}$	|s|

Fourth segment calculation:

Time interval of segment validity: $0 \le t \le \Delta t_{ramp}$

$$\boxed{I_4(t) = I_{exp\_max} + I'(t)_{max} \cdot t}$$

A-1.5. Fifth segment: Parabolic flat top settling

Parabolic settling:		
Given values:		
Initial current of parabola	$I_{endlin} = I_{exp\_max} + \Delta I_{ramp}$	|A|
Current variation during settling parabola	$\Delta I_{p2} = (n\%) * I_{flt}$	|A|
Calculated values:		
Duration of settling parabola	$\Delta t_{p2} = \dfrac{2 \cdot \Delta I_{p2}}{I'(t)_{max}}$	|s|
Current gradient	$\gamma = \dfrac{I'(t)_{max}}{2 \cdot \Delta t_{p2}}$	|A/s²|
Time data for concatenation:		
Absolute starting time	t_{eramp}	|s|
Absolute ending time	$t_{flt} = t_{eramp} + \Delta t_{p2}$	|s|

Fifth segment calculation:

Time interval of segment validity: $\Delta t_{p2} \geq t \geq 0$

$$\boxed{I_5(t) = I_{flt} + \gamma \cdot t^2}$$

After the proper concatenation of these five segments, the shape of the full LHC main dipole proposed baseline current is shown in section 4.